Cell Injury, Repair, Aging, and Apoptosis

Autacoid 14S,21R-Dihydroxy-Docosahexaenoic Acid Counteracts Diabetic Impairment of Macrophage Prohealing Functions

Haibin Tian, Yan Lu, Shraddha P. Shah, and Song Hong

From the Center of Neuroscience Excellence, Louisiana State University Health Sciences Center, New Orleans, Louisiana

Impaired macrophage functions imposed by diabetic complications and the suppressed formation of 14S, 21R-dihydroxydocosa-4Z,7Z,10Z,12E,16Z, 19Z-hexaenoic acid (14S,21R-diHDHA) in wounds contribute significantly to deficient wound healing in diabetics, but how are macrophage functions and 14S,21R-diHDHA formation associated? We studied 14S,21R-diHDHA generation from macrophages using liquid chromatography/mass spectrometry. The role in macrophage-mediated wound healing functions was determined using a murine splinted excisional wound healing model and *in vitro* assays. 14S,21R-diHDHA acts as a macrophage-generated autacoid, and its attenuated formation in macrophages of diabetic *db/db* mice was accompanied by impairment of macrophage prohealing functions. 14S,21R-diHDHA restored *db/db* macrophage-impaired prohealing functions by promoting wound re-epithelialization, formulation of granulation tissue, and vascularization. Additionally, 12/15-lipoxygenase-deficient macrophages, which are unable to produce 14S,21R-diHDHA, exhibited impaired prohealing functions, which also were restored by 14S,21R-diHDHA treatment. The molecular mechanism for 14S,21R-diHDHA-induced recovery of impaired prohealing functions of *db/db* macrophages involves enhancing their secretion of vascular endothelial growth factor and platelet-derived growth factor BB, decreasing hyperglycemia-induced generation of reactive oxygen species, and increasing IL-10 expression under inflammatory stimulation. Taken together, these results indicate that deficiency of 14S,21R-diHDHA formation by diabetic macrophages contributes to their impaired prohealing functions. Our findings provide mechanistic insights into wound healing in diabetics and suggest the possibility of using autologous macrophages/monocytes, treated with 14S,21R-diHDHA, or related compounds, to promote diabetes-impaired wound healing. *(Am J Pathol 2011, 179:1780–1791; DOI: 10.1016/j.ajpath.2011.06.026)*

Impaired wound healing associated with diabetes mellitus presents a major unresolved medical challenge. It is predicted that dysregulated cellular and molecular processes are responsible for impairments in wound healing in diabetes,[1] but the mechanisms underlying these processes require further elucidation. Macrophages play critical roles in wound healing: they engulf apoptotic polymorphonuclear leukocytes (PMNs), tissue debris, and infectious microorganisms; they promote wound healing, including accelerating re-epithelialization by promoting keratinocyte migration from the wound edge to decrease the epithelial gap and increasing the formation of granulation tissue by promoting fibroblasts and endothelial cells moving into wounds to cover the wound bed[2]; and they enhance angiogenesis, to repair damaged blood vessels and thus to supply sufficient oxygen and nutrients during healing.[2] Macrophage prohealing functions have been confirmed: macrophage transplantation into wounds promotes healing,[3,4] and macrophage depletion results in delayed wound healing.[5,6] The presence of diabetes, however, compromises macrophage functions and so contributes to disrupted wound healing.[1,4,7]

In addition to amino acid-based cytokines and growth factors, which are known to mediate wound healing and associated angiogenesis, lipid-derived molecules also may be important mediators. Docosahexaenoic acid (DHA), an essential ω-3 fatty acid, is a relatively abun-

dant, endogenous lipid component in blood and in wounded full-thickness skin.[8] Previous studies showed that DHA can ameliorate diabetes complications, such as cardiovascular disease, by improving endothelial function through anti-inflammatory mechanisms and reduced platelet aggregation, as well as by reducing blood triglyceride levels and increasing high-density lipoprotein cholesterol.[9–11] DHA can also significantly promote wound healing by enhancing angiogenesis.[12] Resolvins, neuroprotectins/protectins, and maresins are lipid mediators generated naturally from DHA during acute inflammation that have potent anti-inflammatory and protective functions.[13,14] Their discovery has opened a new avenue for unraveling the mechanisms behind the beneficial effects of DHA. The DHA-derived lipid mediator neuroprotectin D1 (NPD1; 10R,17S-dihydroxydocosa-4Z,7Z,11E,13E,15Z,19Z-hexaenoic acid) enhances corneal wound healing,[15] and 14S,21R-dihydroxydocosa-4Z,7Z,10Z,12E,16Z,19Z-hexaenoic acid (14S,21R-diHDHA), a novel endogenous DHA-derived lipid mediator, is generated by macrophages and in wounded skin.[8,16] 14S,21R-diHDHA is produced by sequential enzymatic actions of 14S-hydroperoxylation-specific leukocyte-12-lipoxygenase (L-12-LOX) and ω-1-hydroxylation-specific P450.[8] When applied to wounds, 14S,21R-diHDHA potently promotes healing and angiogenesis in wounds.[8,16]

Diabetes and the accompanying hyperglycemia and oxidative stress damage DNA, proteins, and lipids in various tissues. These conditions cause cellular and enzymatic dysfunction during the formation of cytokines and eicosanoids associated with cell growth, angiogenesis, and/or inflammation,[4,7,17–19] all of which are at least in part responsible for impairment of macrophage functions in diabetes.[18,19] We have observed that 14S,21R-diHDHA formation was significantly halted in diabetic wounds, compared with nondiabetic wounds in mice, which suggests that diabetic complications dysregulate the generation of DHA-derived lipid mediators.[16] In addition, supplementation of 14S,21R-diHDHA into diabetic wounds counteracts diabetes-associated impairment of wound healing,[16] indicating that 14S,21R-diHDHA is an important prohealing lipid mediator. Also, decreased 14S,21R-diHDHA formation in diabetes may affect prohealing functions of cells that participate in wound healing.

The findings presented here demonstrate that diabetes-impaired prohealing functions of *db/db* macrophages are associated with decreased formation of 14S,21R-diHDHA, and could be ameliorated by treating diabetic macrophages with 14S,21R-diHDHA.

Materials and Methods

Mice

Animal protocols were approved by the Institutional Animal Care and Use Committee and the Institutional Review Board of the Louisiana State University Health Sciences Center, New Orleans. Studies were blinded. Diabetic *db/db* (BKS.Cg-*m*+/+*Lepr*^db^) and nondiabetic *db/*+ mice (10-week-old females; Jackson Laboratory, Bar Harbor, ME) were used when blood glucose was 22 to 35 mmol/L for *db/db* mice and 5 to 10 mmol/L for *db/*+ mice, as measured with a glucometer. Both B6.129S2-*Alox15*^tm1Fun^/J [12/15 (or leukocyte-12)-lipoxygenase deficient (12/15-LOX^-/-^)] and wild-type control (C57BL/6J) mice were 10-week-old females obtained from the Jackson Laboratory.

Cell Cultures

Macrophages were isolated and identified as previously described.[4,5] Briefly, mice were treated with thioglycolate for 3 days. Macrophages were obtained by peritoneal lavage and were cultured in RPMI 1640 medium (Invitrogen, Carlsbad, CA) containing glucose at different concentrations; nonadherent cells were deleted by changing the culture medium. For identification of macrophages, cells were seeded into eight-well culture slides (BD Biosciences, San Jose, CA). After being fixed in 4% paraformaldehyde (Sigma-Aldrich, St. Louis, MO) for 15 minutes and permeabilized in 0.1% Triton-100 (Sigma-Aldrich) on ice for 5 minutes, cells were incubated with primary antibody (monoclonal rat anti-mouse F4/80; Santa Cruz Biotechnology, Santa Cruz, CA) at 4°C for 12 hours. Cells were then incubated with Cy3-labeled goat anti-rat IgG (Invitrogen) at 4°C for 12 hours. Nuclei were stained with Hoechst 33342 dye (blue). Images were captured using a Zeiss Axioplan 2 microscope in an Everest digital microscopy workstation with associated software (Slidebook version 4.2; Zeiss). More than 95% of cells were F4/80^+^ (see Supplemental Figure S1A at *http://ajp.amjpathol.org*).

Murine fibroblast cell line CF-1 was obtained from the American Type Culture Collection (ATCC, Manassas, VA), and cultured in Dulbecco's modified Eagle's medium containing 10% fetal bovine serum. Dermal microvascular endothelial cells (DMVECs) were isolated from skin of *db/db* mice and confirmed by immunocytochemical analysis, which demonstrated their purity (>95%) based on the staining of endothelial markers CD31 (red) and VE-cadherin (green); nuclei were stained with Hoechst 33342 blue dye (see Supplemental Figure S1B at *http://ajp.amjpathol.org*).[16] Human peripheral blood provided by the New Orleans Blood Bank was collected from a code-deidentified healthy donor who had not taken medication for 2 weeks before donation. Blood was also collected by cardiac puncture from C57BL/6J mice under deep anesthesia.

Polymorphonuclear leukocytes and platelets were separated from human or murine blood as described previously.[20,21] Briefly, peripheral blood samples were mixed with the same volume of PBS containing 4% dextran and were centrifuged at 150 × *g* for 15 minutes. Platelet-rich supernatant was further centrifuged at 1600 × *g* for 15 minutes to collect platelets. Cell deposit was used to isolate PMNs by density gradient centrifugation using Histopaque 1.077 cell separation medium (Sigma-Aldrich). PMNs had at least 95% purity by Hoechst 33342 dye staining and 95% viability by Trypan Blue dye (Sigma-

Aldrich) exclusion. Lymphocytes were isolated from the spleens of *db/+* mice by magnet-based microbead CD45R (B cells) and CD90.2 (T cells) according to the manufacturer's protocol (Miltenyi Biotec, Bergisch Gladbach, Germany). Lymphocytes showed more than 95% viability by Trypan Blue dye exclusion.

Formation of 14S,21R-diHDHA and Its Biosynthetic Intermediates and Analysis by Liquid Chromatography–Ultra Violet Detector–Tandem Mass Spectrometry

The formation of 14S,21R-diHDHA and its biosynthetic intermediates and analysis by liquid chromatography-tandem mass spectrometry were performed as described previously,[8,16] with some modifications. DHA, DHA-d$_5$, and porcine L-12-LOX were supplied by Cayman Chemical (Ann Arbor, MI). Neuroprotectin/protectin D1 (10R,17S-dihydroxy-docosa-4Z,7Z,11E,13E,15Z,19Z-hexaenoic acid) prepared by total organic synthesis was kindly provided by Dr. Charles N. Serhan (Harvard Medical School)[14,22] and Dr. Nicolas G. Bazan (Neuroscience Center of Excellence, Louisiana State University Health Sciences Center, New Orleans).[23] Samples and standards of lipid mediators were handled under dimmed light, stored at −80°C in vials purged with nitrogen gas and sealed tightly. Aqueous solutions of DHA and DHA derivatives were freshly prepared (~4°C) immediately before use.

The separation and analysis of DHA-derived compounds were performed using the liquid chromatography-photodiode array ultra violet detector-linear ion trap mass spectrometer (LC-UV-MS/MS). The LC system was equipped with a chiral column. The mobile phase had a flow-rate of 0.2 mL/min, eluted as B (methanol:H$_2$O: acetic acid = 27:73:0.01) from 0 to 1 minute, ramped from B:methanol 40:60 to B:methanol 20:80 by 50 minutes, ramped to 100% methanol by 55 minutes, and then maintained in 100% methanol. An isotope dilution LC-MS/MS method was used to quantify 14S,21R-diHDHA or mono-HDHAs with 14S,21R-diHDHA-d$_4$ or 14S-hydroxy-DHA-d$_5$ (14S-HDHA-d$_5$) as the internal standard, respectively, which was added to each macrophage sample at the time of collection (10 ng of each standard).[24–28] The UV spectrum was acquired without an internal standard. 14S-HDHA, 14S-HDHA-d$_5$, 14S,21R-diHDHA, or 14S,21R-diHDHA-d$_4$ from the effluent of the chiral LC coupled to the mass spectrometer was analyzed on the basis of selected MS/MS ion chromatograms at a mass-to-charge ratio (m/z) 205 of MS/MS 343, m/z 205 of MS/MS 348, m/z 253 of MS/MS 359, or m/z 253 of MS/MS 363, respectively. The amount of 14S-HDHA or 14S,21R-diHDHA in each macrophage sample was then quantified based on its LC peak area ratio relative to that of its deuterated internal standard 14S-HDHA-d$_5$ or 14S,21R-diHDHA-d$_4$, respectively, using a calibration curve obtained from a series of diluted standards using stable isotope dilution LC-MS/MS method.[24–28]

14S,21R-diHDHA and 14S,21S-diHDHA or their deuterated isotopomers were generated by incubating 14S-HDHA (50 μg) or 14S-HDHA-d$_5$ (50 μg), respectively, with 1 nmol human cytochrome P450 kit (h-P450, containing recombinant human CYP2E1, NADPH cofactor, and buffer salts in the company's proprietary ratios; Codexis-BioCatalytics, Pasadena, CA) (30°C, 12 hours). Under the same conditions, 14R,21R-diHDHA and 14R,21S-diHDHA were generated from 14R-HDHA by h-P450.[8] 14S-HDHA or 14S-HDHA-d$_5$ were prepared by incubating DHA or DHA-d$_5$ (50 μg each), respectively, with porcine L-12-LOX (1000 U) in buffer containing 0.1 mol/L Tris at pH 7.4 for 20 minutes at 37°C. At the end of the incubation, 3 mg of NaBH$_4$ was added.[8,13] Additionally 14S-HDHA and 14R-HDHA were prepared from racemic 14-S/R-HDHAs (Cayman Chemical) by the above chiral LC-UV-MS/MS-based separation. The DHA and 14S-HDHA used to make 14S-HDHA and 14S,21R-diHDHA, respectively, were not less than 98% pure (without detectable oxidation artifacts), as analyzed by chiral LC-UV-MS/MS.

The biosynthesis of 14S,21R-diHDHA and intermediates was assayed by incubating (20 minutes) purified macrophages, PMNs, lymphocytes (T cells/B cells 1:1), fibroblast cells, or DMVECs (1 × 10^7 cells/each type), as well as platelets (1 × 10^8 cells), in PBS containing DHA (3 μmol/L) or 14S-HDHA-d$_5$ (1 μmol/L); this was followed by stimulating the cells (37°C, 1 hour) with TNFα (10 ng/mL), IL-1β (10 ng/mL), and lipopolysaccharide (100 ng/mL). LC-MS/MS analysis indicated that DHA (free acid) in full-thickness murine skin wounds can reach levels as high as 1 to 9 μmol/kg. Thus, 3 μmol/L DHA is within the concentration range found in the pathophysiological condition of skin wounds. TNFα and IL-1β are generated in tissue injury. LPS treatment simulates the potential for infection in wounds.[8,11,29] TNFα, IL-1β, and LPS increase the expression of phospholipase A2, which releases DHA free acid from membranes and/or other parts of the cells. They also likely enhance 12/15-lipoxygenase-like activity,[26] which results in 14-hydroxylation of DHA and some DHA derivatives.[20]

Each incubation was extracted for analysis and preparative separation of 14S,21R-diHDHA or its biosynthetic intermediates. The pH of each incubation was adjusted to pH 4.5 with HCl (1 mol/L, on ice) and then the incubation was mixed with three volumes of ice-cold methanol (sample:methanol = 1:3 v/v). Each mixture was sonicated and centrifuged (4500 × g for 15 minutes at ~4°C). The pellet was extracted with methanol twice. The supernatants for each sample were pooled together and adjusted to 10% methanol with water, and partially purified via C18 solid-phase extraction (500 mg Bond Elut LRC-C18 INT sorbent; Agilent Technologies, Santa Clara, CA). The methanol contained 0.1% butylated hydroxytoluene to suppress auto-oxidation.[28] The final extracts were reconstituted into methanol for chiral LC-UV-MS/MS separation or analysis. For chiral LC preparative separation and fraction collection of compounds generated from incubation, a fraction (10%) of LC flow was split to MS/MS for detection. The fraction of 14S,21R-diHDHA was dried completely with N$_2$ gas and reconstituted in ethanol. The purified 14S,21R-diHDHA and 14S,21R-diHDHA-d$_4$ were found to be not less than 95% pure by LC-UV-MS/MS

using neuroprotectin/protectin-D1[27] as a standard. Additionally, the purified 14S-HDHA-d_5 was quantified by LC-UV-MS/MS using 14-HDHA (Cayman Chemical) as the standard.

Splinted Excisional Wound Healing Model

This model was established as previously described.[16,30,31] Briefly, paired 5-mm circular, full-thickness wounds were made symmetrically along the midline on the dorsal skin of mice. Two days later, 14S,21R-diHDHA (50 ng/wound) or macrophages and 14S,21R-diHDHA-treated macrophages (10^6 cells/wound) were applied to the wound bed (10 µL/bed) and were injected intradermally at four points (10 µL/site) distributed evenly near the wound edge (50 µL total/wound). A donut-shaped silicone splint was adhered around the wound to minimize wound contraction; the splinting did not influence re-epithelialization.[30] This model closely parallels human wound healing. The adherent macrophages were incubated with 100 nmol/L 14S,21R-diHDHA in a dish (37°C, 5% CO_2, 24 hours), resuspended in RPMI 1640 medium, and used as 14S,21R-diHDHA-treated macrophages.

Wound Healing Analysis

Complete re-epithelialization takes ~10 days in wounds of db/db mice and ~7 days in C57BL/6J mice.[16,31,32] To enable quantification of the healing parameters appropriate for our research, re-epithelialization, granulation tissue formation, and angiogenesis were analyzed for wounds at different times for different mice.[16] Briefly, wounds rimmed with 2 mm of unwounded skin were excised from sacrificed mice. Cryosections (10 µm thick) of wounds from db/db mice (day 8 after wounding) and 12/15-LOX$^{-/-}$ or C57BL/6J mice (day 5 after wounding) were analyzed to determine the epithelial gap and granulation tissue formation after H&E staining. The splint has a constant area, and it was used to normalize the wound sizes[30]; therefore, the original epithelial gap (original wound size) was equal in each wound (5 mm in diameter).

The advancing epithelial gap is defined as the distance between the advancing edges of migrated keratinocytes.[30,33] The relative epithelial gap was calculated as a percentage: (advancing epithelial gap/original epithelial gap) × 100. Granulation tissue locates between epidermal layer and subcutaneous layer, and exhibits tight granular morphology. Relative granulation tissue area was calculated as a percentage: (granulation tissue area in treatment/granulation tissue area in control) × 100. Wound vascularity in wounds from db/db mice (day 8 after wounding) and 12/15-LOX$^{-/-}$ or C57BL/6J mice (day 7 after wounding) were assessed by staining vessel endothelial cells with monoclonal rat anti-mouse CD31 antibody followed by goat anti-rat IgG horseradish peroxidase detection kit (BD Biosciences, San Jose, CA), and then by hematoxylin for nuclei. Three to four images per section were captured. Percentage vascularity was calculated as (CD31$^+$ area per field/total wound bed area per field) × 100. Images were captured on a micro-

scope (Zeiss Axio Imager.M1) with an AxioCam MRC camera and Axiovision release 4.6 software. Distance of the epithelial gap, granulation tissue area, and CD31$^+$ area were measured using ImageJ version 1.40 software (NIH, Bethesda, MD).

Macrophage-Conditioned Medium Preparation

Quiescent db/db and db/+ macrophages (3×10^5 cells) were prepared by incubating cells in RPMI 1640 medium containing 25 mmol/L glucose (for 24 hours), and then in fresh RPMI 1640 medium containing 25 mmol/L glucose with or without 100 nmol/L 14S,21R-diHDHA (for 24 hours). The end product, macrophage-conditioned medium (MCM), was collected after centrifugation ($3000 \times g$ for 15 minutes at 4°C).

DMVEC Migration and Vasculature Formation

Analysis of DMVEC migration and vasculature formation was performed as described previously.[16,32] Briefly, quiescent db/db DMVECs were resuspended in RPMI 1640 medium with 25 mmol/L glucose and added to the upper chamber of 24-well Transwell supports (8-µm pore; BD Biosciences) at 1×10^5 cells/well; RPMI 1640 medium with 25 mmol/L glucose or MCM was added to the lower chamber for migration (37°C, 5% CO_2, 4 hours). For vasculature formation, quiescent db/db DMVECs were cultured on Matrigel substrate in a 96-well culture plate (BD Biosciences) at 2×10^4 cells/well in RPMI 1640 medium with 25 mmol/L glucose or MCM (37°C, 5% CO_2, 24 hours). Images were captured on a microscope (Nikon TS100) with a CCD camera and software (NIS-Elements F version 2.30).The vasculature length was measured using NIH ImageJ version 1.40 software.

Bio-Plex Protein Array and Enzyme-Linked Immunosorbent Assay

Vascular endothelial growth factor (VEGF) and platelet-derived growth factor BB (PDGF-BB) secreted by macrophages treated with or without 14S,21R-diHDHA for 24 hours were quantified using a Bio-Plex kit (Bio-Rad, Hercules, CA). In another experiment, quiescent db/db macrophages were treated with 14S,21R-diHDHA with or without LPS for 24 hours. IL-10 in the supernatants was quantified using an enzyme-linked immunosorbent assay kit (Fisher Scientific, Rockford, IL).

Western Blot Analysis

The Western blot experiments were conducted as previously described.[16,34,35] Briefly, The db/db, db/+,12/15-LOX$^{-/-}$ and C57BL/6J peritoneal macrophages were analyzed for 12/15-LOX expression. In another experiment, quiescent macrophages were cultured in RPMI 1640 medium containing 5.5 mmol/L glucose (for db/+, 12/15-LOX$^{-/-}$, and C57BL/6J) or 25 mmol/L glucose (for db/db) with or without 14S,21R-diHDHA and/or IL-4 for 24 hours. Macrophages were analyzed for arginase-1 expres-

sion.[36] Western blot analysis was performed by loading 30 μg total protein/lysed sample to a well in a 4% to 15% Tris-HCl SDS-PAGE gel (Bio-Rad). The electrotransferred protein bands were stained by primary antibodies and then by fluorescent-labeled secondary antibodies (LI-COR, Lincoln, NE), and finally were quantified using a LI-COR Odyssey imaging system.

Reactive Oxygen Species Generation Analysis in Macrophages

Analysis of reactive oxygen species (ROS) generation was performed as described previously.[37] Briefly, The *db/db* and *db/+* macrophages were cultured in RPMI 1640 medium containing 0.1% fetal bovine serum and 5.5 or 25 mmol/L glucose, with or without 100 nmol/L 14*S*,21*R*-diHDHA, for 3 days. Medium was changed every day. ROS generation in cells was assessed using the probe 2,7-dichlorofluorescein diacetate (DCFH-DA, 10 μmol/L; Sigma-Aldrich). Cells were cultured with DCFH-DA in RPMI 1640 medium for 30 minutes and DCFH-DA fluorescence was measured using an excitation wavelength of 480 nm and an emission wavelength of 535 nm.

Statistical Analysis

Statistical analysis was performed using one-way analysis of variance followed by Fisher's least significant difference post hoc comparison. $P < 0.05$ was considered significant.

Results

14S,21R-*diHDHA Formation Is Decreased in Macrophages of Diabetic* db/db *Mice*

To determine effects of diabetes on macrophage production of the prohealing, DHA-derived lipid mediator 14*S*,21*R*-diHDHA[8] and the biosynthetic mechanism, we analyzed 14*S*,21*R*-diHDHA from murine macrophages using a LC-UV-MS/MS (Thermo Fisher Scientific, Waltham, MA) equipped with a chiral column (Chiralpak-IA, 150 mm × 2.1 mm × 5 μm; Chiral Technologies, West Chester, PA). Murine macrophages were isolated from the peritoneal cavity, and 14*S*,21*R*-diHDHA was generated by macrophages in both *db/db* and *db/+* mice (Figure 1). The tandem MS/MS spectrum of peak III (Figure 1A) possessed ions at *m/z* 359 [M-H]⁻, 341 [M-H-H₂O]⁻, 323 [M-H-2H₂O]⁻, 297 [M-H-CO₂-H₂O]⁻, and 279 [M-H-CO₂-2H₂O]⁻, demonstrating two hydroxyl groups and one carboxyl group in the molecular ion *m/z* 359. The 14-hydroxyl was demonstrated by ions *m/z* 205, 233, 189, and 161. The 21-hydroxyl was demonstrated by ions *m/z* 271 and 253, which involved the cleavage of C20-C21 bond in the molecular ion at *m/z* 359 [M-H]⁻ and loss of CH(O)CH₃ (44 atomic units) derived from the terminal group of carbons at the tail of the molecular ion (Figure 1, A and B). Therefore, the peak III compound was 14,21-diHDHA.
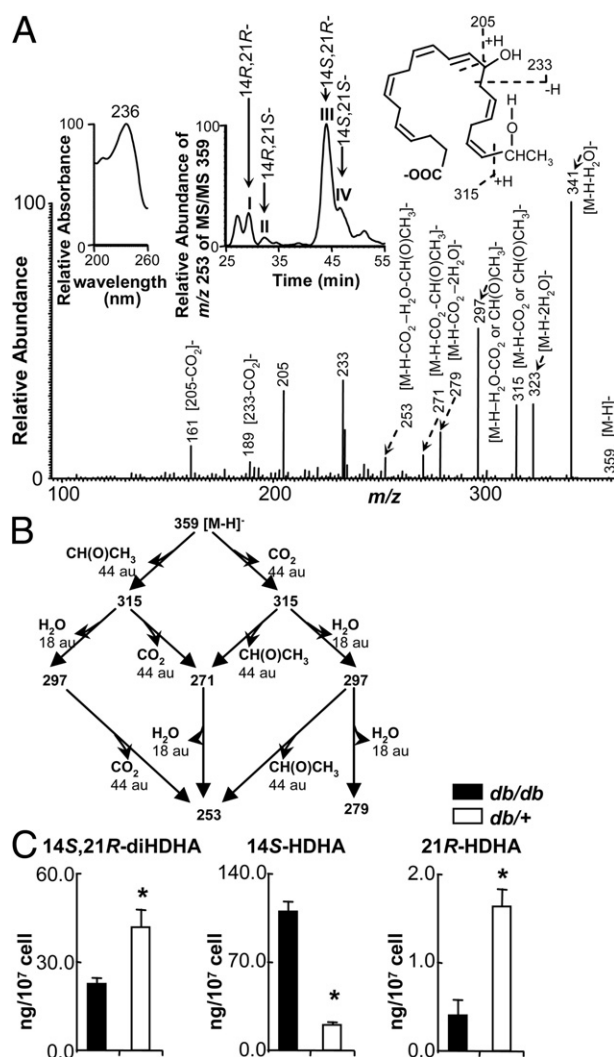

Figure 1. Differences between macrophages from diabetic *db/db* and non-diabetic *db/+* mice in producing 14*S*,21*R*-diHDHA and its biosynthetic intermediates 14*S*-HDHA and 21*R*-diHDHA. Samples were analyzed by Chiralpak-IA-based chiral LC-UV-MS/MS. **A:** 14*S*,21*R*-diHDHA identification (peak III): MS/MS spectrum, UV spectrum (**top left**), MS/MS-based structure elucidation (**top right**), and chiral LC chromatogram (**top middle)** with diastereomers at peak I, II, and IV are annotated. **B:** MS/MS fragmentation pathways for 14*S*,21*R*-diHDHA. **C:** Amount of 14*S*,21*R*-diHDHA, 14*S*-HDHA, or 21*R*-HDHA generated by macrophages (ng/10⁷ cells). Data are reported as means ± SEM (*n* = 3). **P < 0.05.*

There are four 14,21-diHDHA diastereomers resulting from four different combinations of *R/S* configurations of C14 and C21 (14*R,S* and 21*R,S*). The chiral LC retention time of 14,21-diHDHA in peak III (Figure 1A, top middle) matched that of 14*S*,21*R*-diHDHA, which had different retention time than the other three 14,21-diHDHA diastereomers.[16] Therefore, peak III is 14*S*,21*R*-diHDHA. The formation of 14*S*,21*R*-diHDHA was decreased in diabetic *db/db* macrophages, compared with nondiabetic *db/+* macrophages (Figure 1C), based on the chiral LC-MS/MS quantification.

To obtain biochemical insights into the impairment of 14*S*,21*R*-diHDHA biosynthesis in diabetes, we studied the biosynthetic intermediates 14-HDHA and 21-HDHA in *db/db* and *db/+* macrophages.[8] A significantly higher level of 14*S*-HDHA was generated by *db/db* macro-
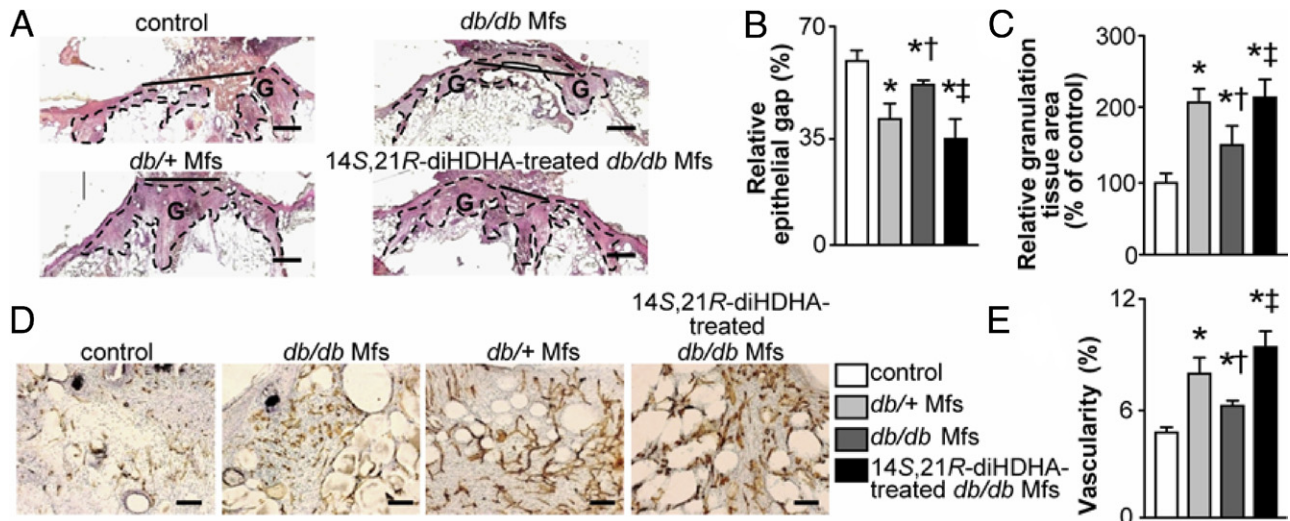
Figure 2. 14S,21R-diHDHA recovers impaired prohealing functions of *db/db* macrophages (Mfs) in cutaneous wounds. Splinted excisional wounds were created in the skin of *db/db* mice. At day 2 after wounding, *db/db* macrophages, 14S,21R-diHDHA-treated *db/db* macrophages, *db/+* macrophages (10^6 cells/wound), or RPMI 1640 vehicle control medium was administered to wounds. Wounded skin was analyzed at day 8 after wounding. **A:** Representative micrographs of H&E-stained cryosections of wounds. A **long black line** marks the epithelial gap; **dashed lines** circumscribe areas of granulation tissue (G). **B:** Relative epithelial gap ($n = 8$). **C:** Relative granulation tissue area ($n = 8$). **D:** Representative microphotographs of CD31$^+$ blood vessels in wounds. **E:** Quantification of wound vascularity ($n = 18$) at day 8 after wounding. Data are reported as means ± SEM. $*P < 0.05$ versus control; $^\dagger P < 0.05$ versus *db/+* macrophage treatment; $^\ddagger P < 0.05$ versus *db/db* macrophage treatment. Scale bars, 500 μm (**A**); 100 μm (**D**).

phages, compared with *db/+* macrophages (Figure 1C). This coincided with up-regulated expression of L-12-LOX (see Supplemental Figure S2A at *http://ajp.amjpathol. org*), which is involved in DHA 14S-hydroxylation. However, the 21R-HDHA level was significantly lower in *db/db* macrophages than in *db/+* macrophages (Figure 1C), which suggests that diabetes may impede 14S,21R-diHDHA biosynthesis by interfering with 21-hydroxygenation.[8]

We studied the 14S,21R-diHDHA biosynthesis in selected typical types of cells that are known to participate in wound healing.[2] The results from our chiral LC-MS/MS analysis show that PMNs, platelets, and skin cells (including fibroblasts and DMVECs) did not produce 14S,21R-diHDHA; whereas lymphocytes (T cells and B cells) produced a much lesser amount of 14S,21R-diHDHA, compared with macrophages, and platelets produced the intermediate 14S-HDHA for the biosynthesis of 14S,21R-diHDHA (Figure 1A; see also Supplemental Figure S3 at *http://ajp.amjpathol.org*). These data suggest that macrophages produce 14S,21R-diHDHA in wounds, especially at days 2 to 4 after wounding, when macrophages are the major leukocytes in wounds.[2] These results motivated us to further study the relation of decreased generation of 14S,21R-diHDHA to impaired prohealing functions of diabetic macrophages.

14S,21R-diHDHA Recovers Impaired Prohealing Functions of Macrophages of Diabetic db/db Mice

To determine whether the impaired prohealing functions of *db/db* macrophages is associated with decreased 14S,21R-diHDHA generation, *db/+*, *db/db* macrophages and 14S,21R-diHDHA-treated *db/db* macrophages were

injected into wounds of *db/db* mice at day 2 after wounding, when considerable numbers of endogenous macrophages are recruited in the natural course of wound healing.[1,2] Compared with vehicle controls, the administration of *db/+* macrophages or *db/db* macrophages significantly promoted re-epithelialization by decreasing the epithelial gap and increasing formation of granulation tissue (Figure 2, A–C). In addition, *db/db* macrophages showed impaired functions in accelerating wound healing, compared with *db/+* macrophages (Figure 2, A–C), which is consistent with a previous report.[4] 14S,21R-diHDHA-treated *db/db* macrophages considerably decreased the epithelial gap and increased granulation tissue area, compared with *db/db* macrophage treatment (Figure 2, A–C). These results provide evidence that reduced generation of 14S,21R-diHDHA in diabetic *db/db* macrophages contributed to impaired prohealing functions, and that these functions were restored by 14S,21R-diHDHA treatment.

Impaired angiogenesis is a critical hallmark of nonhealing wounds in diabetes.[1] Our data demonstrate that wounds of *db/db* mice injected with *db/+* or *db/db* macrophages exhibited increased vascularity, compared with wounds of control animals (Figure 2, D and E). In addition, significantly more CD31$^+$ vessels were found in the wound beds injected with 14S,21R-diHDHA-treated *db/db* macrophages than with untreated *db/db* macrophages (Figure 2, D and E). Indeed, untreated *db/db* macrophages were less efficient than *db/+* macrophages in promoting angiogenesis (Figure 2, D and E). Thus, 14S,21R-diHDHA counteracted diabetes impairment and recovered macrophage prohealing functions, including enhanced angiogenesis.

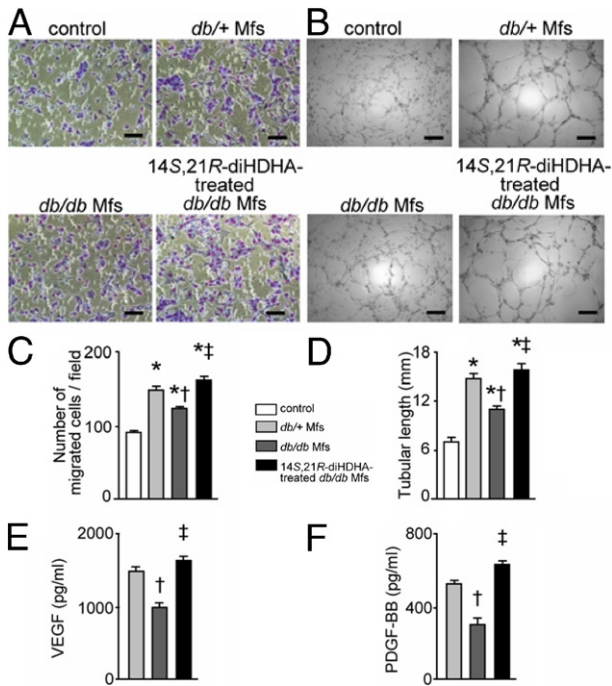To further understand the cellular mechanism by which 14S,21R-diHDHA rescues impaired macrophage pro-

Figure 3. 14*S*,21*R*-diHDHA treatment restores *db/db* macrophage function in cellular processes of angiogenesis in *db/db* DMVECs. Representative micrographs of DMVEC migration (**A**) and vasculature formation (**B**) in RPMI 1640 vehicle control medium or in MCM. Data are quantified as migrated DMVECs per field (*n* = 15) (**C**) and as vasculature length per field (*n* = 4) (**D**). VEGF (**E**) and PGDF-BB (**F**) secreted from *db/db* macrophages, 14*S*,21*R*-diHDHA-treated *db/db* macrophages, or *db/+* macrophages were measured using a Bio-Plex protein array (*n* = 3). Scale bars = 100 μm. Data are reported as means ± SEM. *$P < 0.05$ versus control; ‡$P < 0.01$ versus *db/+* MCM; ‡$P < 0.05$ versus *db/db* MCM.

healing functions in diabetes, we studied diabetic *db/db* DMVEC migration and vasculature formation in MCM. Media conditioned by *db/+* and *db/db* macrophages considerably increased *db/db* DMVEC migration and enhanced vasculature formation, compared with controls (non-MCM) (Figure 3, A–D). The *db/db* MCM was significantly less effective in promoting *db/db* DMVEC migration and vasculature formation, compared with *db/+* MCM, demonstrating that macrophage functions in angiogenesis were impaired in diabetic mice. When conditioned medium from 14*S*,21*R*-diHDHA-treated *db/db* macrophages was used, *db/db* DMVEC migration and vasculature formation was significantly enhanced, relative to *db/db* MCM (Figure 3, A–D). These data indicate that 14*S*,21*R*-diHDHA enhanced functions of *db/db* macrophages in angiogenesis through promoting DMVEC migration and vasculature formation.

Macrophages promote angiogenesis by secreting angiogenic cytokines such as VEGF and PDGF-BB.[1,2,38] We postulated, therefore, that 14*S*,21*R*-diHDHA enhances the functions of *db/db* macrophages in angiogenesis, in part, by increasing their angiogenic cytokine production. The results demonstrated that lesser amounts of VEGF and PDGF-BB were released by *db/db* macrophages than by *db/+* macrophages (Figure 3, E and F), consistent with impaired functions of *db/db* macrophages. This impairment was diminished by 14*S*,21*R*-diHDHA, which activated *db/db* macrophages to secrete

significantly more VEGF and PDGF-BB under simulated hyperglycemia (Figure 3, E and F). Taken together, these results suggest that 14*S*,21*R*-diHDHA treatment restored the impaired prohealing functions of *db/db* macrophages in angiogenesis by enhancing *db/db* macrophage paracrine capacity.

12/15-LOX$^{-/-}$ Macrophages Exhibit Impaired Prohealing Functions Associated with Decreased 14S,21R-diHDHA Biosynthesis

To further confirm that endogenous 14*S*,21*R*-diHDHA positively regulated macrophage prohealing functions, 12/15-LOX$^{-/-}$ macrophages were compared with wild-type C57BL/6J macrophages. We found that 12/15-LOX$^{-/-}$ macrophages did not produce 14*S*,21*R*-diHDHA, whereas macrophages from C57BL/6J, BALB/c, *db/db*, or *db/+* mice did[8,16] (Figure 1A). This finding was expected, because 12/15-LOX is the only LOX available in macrophages that catalyzes the 14*S*-hydroperoxylation step[39] in 14*S*,21*R*-diHDHA biosynthetic pathways and 12/15-LOX could not be detected in 12/15-LOX$^{-/-}$ macrophages. After injection into wounds, C57BL/6J macrophages significantly promoted re-epithelialization with a decreased epithelial gap and promoted granulation tissue formation, as shown by an augmented granulation tissue area, compared with vehicle control (Figure 4, A–C). 12/15-LOX$^{-/-}$ macrophages had no effect on re-epithelialization, but they did cause a slight increase in granulation tissue formation (Figure 4, A–C). Thus, 12/15-LOX$^{-/-}$ macrophages exhibited impaired functions in accelerating wound healing, compared with C57BL/6J macrophages (see Supplemental Figure S2 at *http://ajp.amjpathol.org*). After treatment with 14*S*,21*R*-diHDHA, 12/15-LOX$^{-/-}$ macrophages significantly accelerated wound healing. 14*S*,21*R*-diHDHA-treated 12/15-LOX$^{-/-}$ macrophages decreased the epithelial gap and increased granulation tissue area, compared with untreated 12/15-LOX$^{-/-}$ macrophages (Figure 4, A–C).

The effect of decreased 14*S*,21*R*-diHDHA production on macrophage functions for angiogenesis was further addressed. We found that wounds injected with 12/15-LOX$^{-/-}$ macrophages did not exhibit increased vascularity, relative to the control, and also had much less vascularity relative to C57BL/6J macrophage treatment (Figure 4, D and E). However, significantly higher wound vascularity was found in wounds injected with 14*S*,21*R*-diHDHA-treated 12/15-LOX$^{-/-}$ macrophages than in wounds injected with untreated 12/15-LOX$^{-/-}$ macrophages (Figure 4, D and E). Thus, impaired prohealing functions of 12/15-LOX$^{-/-}$ macrophages are associated with decreased biosynthesis of 14*S*,21*R*-diHDHA.

Given that i) macrophages are the main leukocytes, ii) there are relatively fewer PMNs in wounds at days 2 to 3 after wounding, and iii) macrophages produce 14*S*,21*R*-diHDHA, we wanted to clarify whether application of 14*S*,21*R*-diHDHA can ameliorate wound healing after macrophages become the dominant leukocytes. Wound healing in 12/15-LOX$^{-/-}$ mice was compared
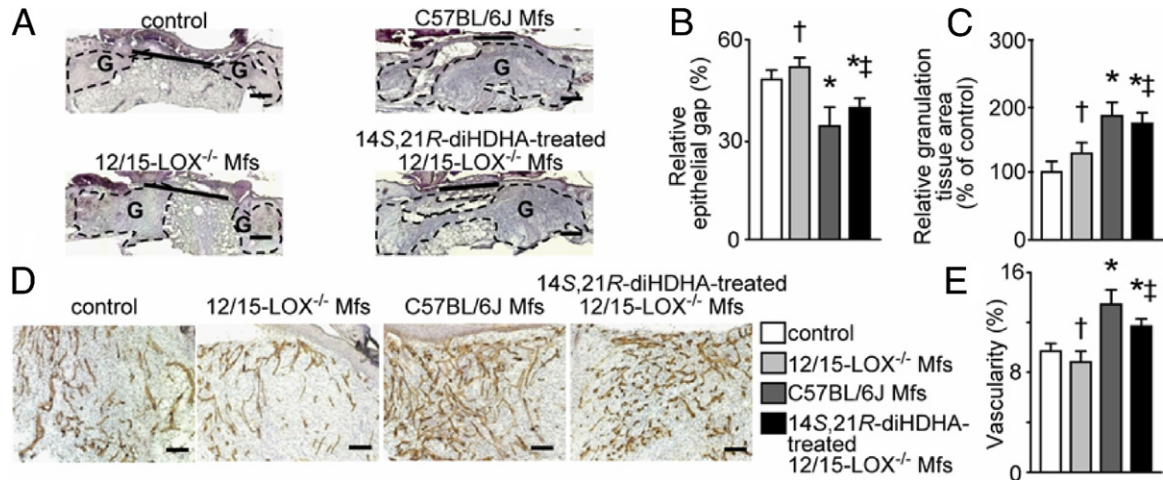
Figure 4. 14S,21R-diHDHA treatment restores macrophage prohealing functions impaired by 12/15-LOX deficiency. Splinted excisional wounds were created in the skin of C57BL/6J mice. Wounds were then treated with vehicle control, 12/15-LOX$^{-/-}$ macrophages, 14S,21R-diHDHA-treated 12/15-LOX$^{-/-}$ macrophages, or C57BL/6J macrophages (10^6 cells/wound) at day 2 after wounding. **A:** Representative micrographs of H&E-stained cryosections of wounded skin collected at day 5 after wounding. A **long black line** marks the epithelial gap; **dashed lines** circumscribe areas of granulation tissue (G). **B:** Relative epithelial gap ($n = 8$). **C:** Relative granulation tissue area ($n = 8$). **D:** Representative microphotographs of CD31$^+$ blood vessels in wounds. **E:** Quantification of wound vascularity ($n = 18$) at day 7 after wounding. Data are reported as means ± SEM. *$P < 0.05$ versus control; †$P < 0.05$ versus C57BL/6J macrophage treatment; ‡$P < 0.05$ versus 12/15-LOX$^{-/-}$ macrophage treatment. Scale bars, 500 μm (**A**); 100 μm (**D**).

with that in wild-type C57BL/6J mice. Previous data showed decreased 14S,21R-diHDHA formation in wounds of 12/15-LOX$^{-/-}$ mice, compared with wounds of C57BL/6J mice.[16] In addition, correlative with diminished formation of 14S,21R-diHDHA, histological analysis showed that 12/15-LOX$^{-/-}$ mice exhibited impaired cutaneous wound healing, compared with C57BL/6J mice, as well as delayed re-epithelialization (Figure 5, A and B), decreased granulation tissue formation (Figure 5, A and C), and decreased vascularity (Figure 5, D and E). Application of 14S,21R-diHDHA into wounds of 12/15-LOX$^{-/-}$ mice at day 2 after wounding significantly promoted re-epithelialization and granulation tissue formation, as well as vascularity (Figure 5). These data suggest that 14S,21R-diHDHA may ame-

liorate wound healing through modulating macrophage functions.

14S,21R-diHDHA Reduces Generation of ROS and Increases IL-10 Expression in db/db Macrophages

Oxidative stress is a critical cause for impaired macrophage functions in diabetes.[18,19] We therefore investigated whether 14S,21R-diHDHA treatment reduces ROS generation. A high concentration of glucose (25 mmol/L) induced ROS generation in db/+ macrophages. A low glucose concentration (5.5 mmol/L) resulted in slightly decreased ROS generation in db/db macrophages
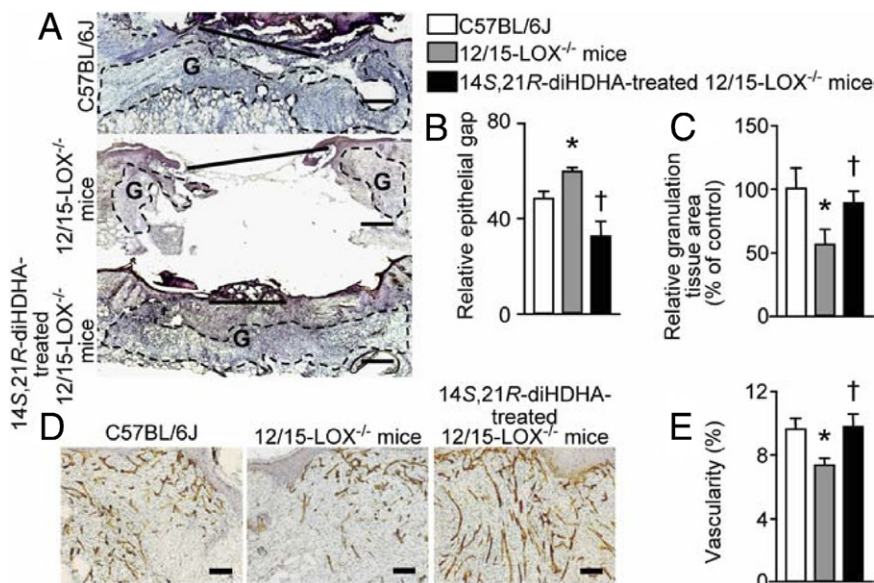

Figure 5. 14S,21R-diHDHA ameliorates impaired cutaneous wound healing in 12/15-LOX$^{-/-}$ mice. Splinted excisional wounds were made in the skin of 12/15-LOX$^{-/-}$ mice and C57BL/6J mice. Wounds were then treated with 14S,21R-diHDHA (50 ng/wound) at day 2 after wounding. Wounds of C57BL/6J mice received only vehicle. **A:** Representative micrographs of H&E-stained cryosections of wounds at day 5 after wounding. A **long black line** marks the epithelial gap; **dashed lines** circumscribe areas of granulation tissue (G). **B:** Relative epithelial gap ($n = 8$). **C:** Relative granulation tissue area ($n = 8$). **D:** Representative microphotographs of CD31$^+$ blood vessels in wounds. **E:** Quantification of wound vascularity ($n = 18$) at day 7 after wounding. Data are reported as means ± SEM. *$P < 0.05$ versus C57BL/6J mice; †$P < 0.05$ compared 12/15-LOX$^{-/-}$ mice treated with vehicle control. Scale bars, 500 μm (**A**); 100 μm (**D**).
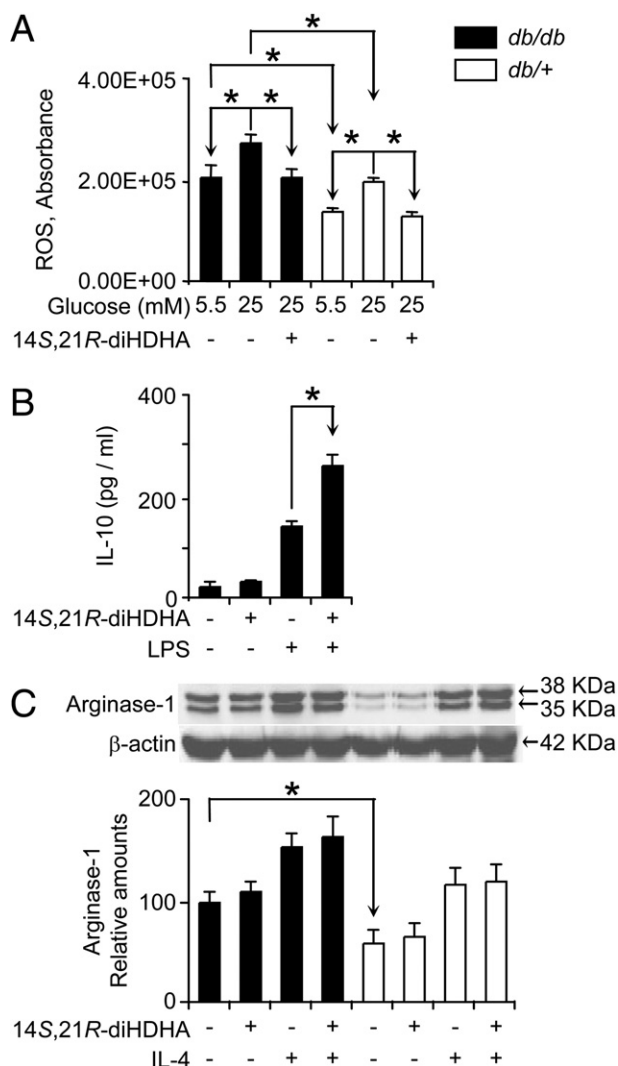
A

B

C

Figure 6. 14*S*,21*R*-diHDHA reduces ROS generation induced by high concentrations of glucose and increases IL-10 expression in *db/db* macrophages under LPS stimulation. **A:** ROS generation. *db/db* and *db/+* macrophages were cultured in 5.5 mmol/L or 25 mmol/L glucose and treated with 14*S*,21-diHDHA. ROS generation in cells was assessed using the probe DCFH-DA (*n* = 4). **B:** IL-10 expression. IL-10 secreted from *db/db* macrophages treated with 14*S*,21*R*-diHDHA, LPS, or 14*S*,21*R*-diHDHA plus LPS was measured using an IL-10 enzyme-linked immunosorbent assay kit (*n* = 3). **C:** Arginase-1 expression. Quiescent *db/db* and *db/+* macrophages were cultured for 24 hours in RPMI 1640 medium with 14*S*,21*R*-diHDHA, IL-4, or both IL-4 and 14*S*,21*R*-diHDHA. Macrophage lysates were analyzed by Western blot. Arginase-1 quantities relative to *β*-actin were measured based on optical densities of the gel bands and were normalized to that of nontreated *db/db* macrophages (*n* = 3). 14*S*,21*R*-diHDHA, 100 nmol/L; IL-4, 10 ng/mL; LPS, 100 ng/mL. Data are reported as means ± SEM. *$P < 0.05$.

(Figure 6A). The *db/db* macrophages produced more ROS, compared with *db/+* macrophages (Figure 6A). 14*S*,21*R*-diHDHA treatment decreased ROS generation by *db/+* and *db/db* macrophages in high-glucose conditions (Figure 6A). Thus, 14*S*,21*R*-diHDHA may affect macrophage function by reducing ROS generation under high-glucose conditions.

IL-10 is an important anti-inflammatory cytokine up-regulated by LPS.[29] LPS stimulation resembles the potential of infection to wounds. To determine the effect of 14*S*,21*R*-diHDHA on IL-10 expression, we treated *db/db* macrophages with 14*S*,21*R*-diHDHA alone, 14*S*,21*R*-

diHDHA plus LPS, LPS alone, or vehicle control. We found that 14*S*,21*R*-diHDHA significantly promoted LPS-induced IL-10 generation by macrophages, although 14*S*,21*R*-diHDHA alone did not affect IL-10 generation by *db/db* macrophages (Figure 6B). These results indicate that 14*S*,21*R*-diHDHA enhanced the anti-inflammatory functions of *db/db* macrophages. We also assessed the effect of 14*S*,21*R*-diHDHA on IL-4-induced alternative activation,[40] which results in a prohealing phenotype in macrophages and characteristically involves arginase-1 expression. 14*S*,21*R*-diHDHA did not affect this type of activation of macrophages under the *in vitro* conditions used in the present study (Figure 6C).

Discussion

Wound healing is a dynamic process that is characterized by inflammation, tissue regeneration, and remodeling.[2] We have observed that wounded skin can generate 14*S*,21*R*-diHDHA.[8,16] Several kinds of cells contribute to wound healing.[2] Our data show that macrophages possess a greater capability to produce 14*S*,21*R*-diHDHA, compared with several other typical cell types usually present in wounds. 14*S*,21*R*-diHDHA formation was reduced in diabetic *db/db* macrophages, compared with nondiabetic *db/+* macrophages (Figure 1), which suggests that diabetes dysregulation of macrophage biosynthesis of 14*S*,21*R*-diHDHA could contribute to diabetes impairment of 14*S*,21*R*-diHDHA production in diabetic wounds.[16] The formation of 14*S*-HDHA, a marker of 12-LOX activity,[8] was elevated in diabetic wounds. Nevertheless, the decreased 21*R*-HDHA formation (Figure 1) suggests that diabetes attenuates 21*R*-hydroxylation, which could contribute to reduced 14*S*,21*R*-diHDHA generation. The 21*R*-hydroxylation is likely to be catalyzed by a specific P450[41] in macrophages,[8,42] which is of interest for our future studies.

Diabetic hyperglycemia and accompanying oxidative stress might affect biosynthesis of 14*S*,21*R*-diHDHA by altering P450 or disrupting the transfer of biosynthetic intermediates[8] between 12-LOX and P450 within or between cells. 12/15-LOX$^{-/-}$ macrophages are deficient in 14*S*,21*R*-diHDHA generation; we therefore used 12/15-LOX$^{-/-}$ macrophages as negative control to study the role of this autacoid-type mediator in macrophage functions. Although platelets are unable to produce 14*S*,21*R*-diHDHA, and lymphocytes barely produce this mediator, both cell types produce the intermediate 14*S*-HDHA of 14*S*,21*R*-diHDHA biosynthesis (see Supplemental Figure S3 at *http://ajp.amjpathol.org*). The 14*S*-HDHA produced by platelets or lymphocytes was likely transported to macrophages and there converted to 14*S*,21*R*-diHDHA through the transcellular biosynthesis mechanism for lipid mediators.[43,44]

Macrophages are the main leukocytes in wounds at days 2 to 3 after wounding, when the wounds are still in the inflammation phase.[2] They are activated to phagocytose apoptotic PMNs, debris, and bacteria, and then coordinate later events of healing, including re-epithelialization, granulation tissue formation, and angiogenesis.
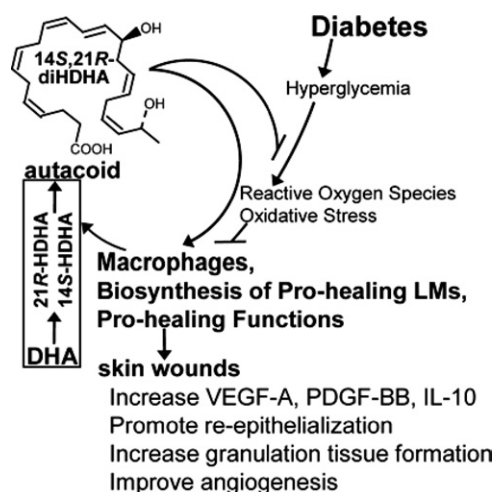
Figure 7. Impairment of prohealing functions of diabetic *db/db* macrophages is associated with reduced 14S,21R-diHDHA formation. Diabetes decreases the generation of 14S,21R-diHDHA by macrophages. Treatment with 14S,21R-diHDHA rescues diabetes-impaired macrophage promotion of wound re-epithelialization, granulation tissue formation, and vascularization. The mechanism of 14S,21R-diHDHA action on macrophages includes reducing ROS generation under hyperglycemia, increasing IL-10 expression, increasing the secretion of VEGF and PDGF-BB, and enhancing the macrophage promotion of endothelial cell migration and vasculature formation.

Impaired macrophage functions are among the crucial defects responsible for delayed wound healing in diabetics. Compared with normal macrophages, diabetic macrophages display detrimental pathophysiological responses, such as expressing low levels of angiogenic cytokines,[4,17–19] including reduced expression of VEGF and PDGF-BB (Figure 3). Moreover, the association of decreased formation of 14S,21R-diHDHA with impaired prohealing functions of *db/db* macrophages indicates that impaired functions of diabetic macrophages also includes impaired formation of this autacoid. This association was further confirmed by the fact that 12/15-LOX$^{-/-}$ macrophages could not produce 14S,21R-diHDHA and exhibited attenuated promotion of healing that could be restored by 14S,21R-diHDHA treatment (Figure 4). Impaired functions of 12/15-LOX$^{-/-}$ macrophages may not only result from halted 14S,21R-diHDHA formation, but may also stem from other detrimental effects of 12/15-LOX deletion; however, 14S,21R-diHDHA treatment can restore macrophage functions, indicating that 14S,21R-diHDHA can redeem those effects. Additionally, 12/15-LOX$^{-/-}$ mice exhibiting delayed wound healing. The application of 14S,21R-diHDHA at day 2 after wounding, when macrophages significantly infiltrate into wounds, counteract such impairment (Figure 5). This further suggests the reparative roles of 14S,21R-diHDHA via action on macrophages in wounds. However, the paracrinic action of macrophage 14S,21R-diHDHA on other kinds of cells in wounds cannot be excluded and should be investigated in future studies.

During the inflammatory phase of wound repair, ROS generated by PMNs and macrophages destroy harmful microorganisms and stimulate expression of some growth factors.[45] However, overproduction of ROS leads to excessive oxidative stress and results in cellular dysfunction and functional alterations of DNA, lipids, and proteins.[17,45,46] The high glucose concentration in diabetic hyperglycemia is a critical initiating factor for ROS generation.[47] In this regard, *db/db* macrophages generated much more ROS than *db/+* macrophages, which is consistent with a previous report.[18] High glucose concentrations induce significant increases in ROS production in macrophages (Figure 6). Thus, diabetic hyperglycemia might stimulate macrophages to produce excessive ROS, which cause macrophage dysfunction. Moreover, the suppression of oxidative stress has been shown to reduce the abnormally high levels of proinflammatory cytokines in diabetic macrophages.[19] 14S,21R-diHDHA was found to decrease ROS generation (Figure 6), providing another possible means by which 14S,21R-diHDHA treatment mediates recovery of macrophage prohealing functions in diabetes.

Heterogeneity of macrophages has recently been proposed. Alternatively activated macrophages, as distinct from classically activated macrophages, promote wound healing, and macrophages are capable of switching phenotypes under different stimuli.[40] However, 14S,21R-diHDHA did not affect arginase-1 expression under IL-4 stimulus (Figure 6), a property of alternatively activated macrophages, suggesting that 14S,21R-diHDHA does not act on the macrophage switching to an alternative phenotype. 14S,21R-diHDHA increased IL-10 expression by *db/db* macrophages under LPS stimulation (Figure 6), suggesting that the recovery of diabetic prohealing functions by 14S,21R-diHDHA may involve augmenting IL-10 generation. Of note, *db/db* macrophages expressed more arginase-1, compared with *db/+* macrophages (Figure 6). Arginase-1 effectively competed with nitric oxide synthase for arginine and converted arginine to urea and ornithine, thus preventing the overproduction of nitric oxide.[48] Increased expression of arginase-1 and IL-10 in *db/db* macrophages, compared with *db/+* macrophages, may be an adaptive response under the stress of diabetes.[49]

The DHA-derived lipid mediator 14S,21R-diHDHA acts as an macrophage-produced autacoid that promotes the prohealing functions of macrophages (Figure 7). Reduced formation of 14S,21R-diHDHA in *db/db* macrophages is associated with their impaired prohealing functions. 14S,21R-diHDHA treatment of macrophages reduced ROS generation, promoted IL-10 generation, and enhanced diabetic macrophage prohealing functions. These observations provide mechanistic insights into wound healing and point toward possible treatment of wounds in diabetic patients using autologous macrophages treated with 14S,21R-diHDHA or related compounds.

and Dr. Qiang Wu and Jose A. Galindo for technical assistance.

References

1. Falanga V: Wound healing and its impairment in the diabetic foot. Lancet 2005, 366:1736–1743
2. Broughton G 2nd, Janis JE, Attinger CE: The basic science of wound healing. Plast Reconstr Surg 2006, 117:12S–34S
3. Danon D, Kowatch MA, Roth GS: Promotion of wound repair in old mice by local injection of macrophages. Proc Natl Acad Sci USA 1989, 86:2018–2020
4. Maruyama K, Asai J, Ii M, Thorne T, Losordo DW, D'Amore PA: Decreased macrophage number and activation lead to reduced lymphatic vessel formation and contribute to impaired diabetic wound healing. Am J Pathol 2007, 170:1178–1191
5. Lucas T, Waisman A, Ranjan R, Roes J, Krieg T, Müller W, Roers A, Eming SA: Differential roles of macrophages in diverse phases of skin repair. J Immunol 2010, 184:3964–3977
6. Mirza R, DiPietro LA, Koh TJ: Selective and specific macrophage ablation is detrimental to wound healing in mice. Am J Pathol 2009, 175:2454–2462
7. Khanna S, Biswas S, Shang Y, Collard E, Azad A, Kauh C, Bhasker V, Gordillo GM, Sen CK, Roy S: Macrophage dysfunction impairs resolution of inflammation in the wounds of diabetic mice. PLoS One 2010, 5:e9539
8. Lu Y, Tian H, Hong S: Novel 14,21-dihydroxy-docosahexaenoic acids: structures, formation pathways, and enhancement of wound healing. J Lipid Res 2010, 51:923–932
9. Abbatecola AM, Evans W, Paolisso G: PUFA supplements and type 2 diabetes in the elderly. Curr Pharm Des 2009, 15:4126–4134
10. Nettleton JA, Katz R: n-3 Long-chain polyunsaturated fatty acids in type 2 diabetes: a review. J Am Diet Assoc 2005, 105:428–440
11. Montori VM, Farmer A, Wollan PC, Dinneen SF: Fish oil supplementation in type 2 diabetes: a quantitative systematic review. Diabetes Care 2000, 23:1407–1415
12. Shingel KI, Faure MP, Azoulay L, Roberge C, Deckelbaum RJ: Solid emulsion gel as a vehicle for delivery of polyunsaturated fatty acids: implications for tissue repair, dermal angiogenesis and wound healing. J Tissue Eng Regen Med 2008, 2:383–393
13. Serhan CN, Yang R, Martinod K, Kasuga K, Pillai PS, Porter TF, Oh SF, Spite M: Maresins: novel macrophage mediators with potent antiinflammatory and proresolving actions. J Exp Med 2009, 206:15–23
14. Hong S, Gronert K, Devchand PR, Moussignac RL, Serhan CN: Novel docosatrienes and 17S-resolvins generated from docosahexaenoic acid in murine brain, human blood, and glial cells. Autacoids in anti-inflammation. J Biol Chem 2003, 278:14677–14687
15. Gronert K, Maheshwari N, Khan N, Hassan IR, Dunn M, Laniado Schwartzman M: A role for the mouse 12/15-lipoxygenase pathway in promoting epithelial wound healing and host defense. J Biol Chem 2005, 280:15267–15278
16. Tian H, Lu Y, Shah SP, Hong S: 14S,21R-Dihydroxydocosahexaenoic acid remedies impaired healing and mesenchymal stem cell functions in diabetic wounds. J Biol Chem 2011, 286:4443–4453
17. Brownlee M: Biochemistry and molecular cell biology of diabetic complications. Nature 2001, 414:813–820
18. Ptak W, Klimek M, Bryniarski K, Ptak M, Majcher P: Macrophage function in alloxan diabetic mice: expression of adhesion molecules, generation of monokines and oxygen and NO radicals. Clin Exp Immunol 1998, 114:13–18
19. Haskins K, Bradley B, Powers K, Fadok V, Flores S, Ling X, Pugazhenthi S, Reusch J, Kench J: Oxidative stress in type 1 diabetes. Ann NY Acad Sci 2003, 1005:43–54
20. Tian H, Lu Y, Sherwood AM, Hongqian D, Hong S: Resolvins E1 and D1 in choroid-retinal endothelial cells and leukocytes: biosynthesis and mechanisms of anti-inflammatory actions. Invest Ophthalmol Vis Sci 2009, 50:3613–3620
21. Dona M, Fredman G, Schwab JM, Chiang N, Arita M, Goodarzi A, Cheng G, von Andrian UH, Serhan CN: Resolvin E1, an EPA-derived mediator in whole blood, selectively counterregulates leukocytes and platelets. Blood 2008, 112:848–855
22. Serhan CN, Gotlinger K, Hong S, Lu Y, Siegelman J, Baer T, Yang R, Colgan SP, Petasis NA: Anti-inflammatory actions of neuroprotectin D1/protectin D1 and its natural stereoisomers: assignments of dihydroxy-containing docosatrienes [Erratum appeared in J Immunol 2006, 176:3843]. J Immunol 2006, 176:1848–1859
23. Marcheselli VL, Hong S, Lukiw WJ, Tian XH, Gronert K, Musto A, Hardy M, Gimenez JM, Chiang N, Serhan CN, Bazan NG: Novel docosanoids inhibit brain ischemia-reperfusion-mediated leukocyte infiltration and pro-inflammatory gene expression [Erratum appeared in J Biol Chem 2003, 278:51974]. J Biol Chem 2003, 278:43807–43817
24. Basselin M, Kim HW, Chen M, Ma K, Rapoport SI, Murphy RC, Farias SE: Lithium modifies brain arachidonic and docosahexaenoic metabolism in rat lipopolysaccharide model of neuroinflammation. J Lipid Res 2010, 51:1049–1056
25. Yang P, Chan D, Felix E, Madden T, Klein RD, Shureiqi I, Chen X, Dannenberg AJ, Newman RA: Determination of endogenous tissue inflammation profiles by LC/MS/MS: COX- and LOX-derived bioactive lipids. Prostaglandins Leukot Essent Fatty Acids 2006, 75:385–395
26. Gronert K, Clish CB, Romano M, Serhan CN: Transcellular regulation of eicosanoid biosynthesis. Methods Mol Biol 1999, 120:119–144
27. Bazan NG, Marcheselli VL, Lu Y, Hong S, Jackson F: Lipidomic approaches to neuroprotection signaling in the retinal pigment epithelium. Signal Transduction in the Retina. Edited by SJ Fliesler, OG Kisselev. Boca Raton, FL, CRC Press, 2008, pp 349–374
28. Hall LM, Murphy RC: Electrospray mass spectrometric analysis of 5-hydroperoxy and 5-hydroxyeicosatetraenoic acids generated by lipid peroxidation of red blood cell ghost phospholipids. J Am Soc Mass Spectrom 1998, 9:527–532
29. Barsness KA, Bensard DD, Partrick DA, Calkins CM, Hendrickson RJ, McIntyre RC Jr: Endotoxin induces an exaggerated interleukin-10 response in peritoneal macrophages of children compared with adults. J Pediatr Surg 2004, 39:912–915; discussion 912–915
30. Galiano RD, Michaels J 5th, Dobryansky M, Levine JP, Gurtner GC: Quantitative and reproducible murine model of excisional wound healing. Wound Repair Regen 2004, 12:485–492
31. Michaels J 5th, Churgin SS, Blechman KM, Greives MR, Aarabi S, Galiano RD, Gurtner GC: db/db mice exhibit severe wound-healing impairments compared with other murine diabetic strains in a silicone-splinted excisional wound model. Wound Repair Regen 2007, 15:665–670
32. Tian H, Lu Y, Shah SP, Hong S: Novel 14S,21-dihydroxy-docosahexaenoic acid rescues wound healing and associated angiogenesis impaired by acute ethanol intoxication/exposure. J Cell Biochem 2010, 111:266–273
33. Stepanovic V, Awad O, Jiao C, Dunnwald M, Schatteman GC: Leprdb diabetic mouse bone marrow cells inhibit skin wound vascularization but promote wound healing. Circ Res 2003, 92:1247–1253
34. Gee E, Milkiewicz M, Haas TL: p38 MAPK activity is stimulated by vascular endothelial growth factor receptor 2 activation and is essential for shear stress-induced angiogenesis. J Cell Physiol 2010, 222:120–126
35. Sharma GD, HE J, Bazan HE: p38 and ERK1/2 coordinate cellular migration and proliferation in epithelial wound healing: evidence of cross-talk activation between MAP kinase cascades. J Biol Chem 2003, 278:21989–21997
36. Louis CA, Mody V, Henry WL Jr, Reichner JS, Albina JE: Regulation of arginase isoforms I and II by IL-4 in cultured murine peritoneal macrophages. Am J Physiol 1999, 276:R237–R242
37. Ali MH, Schlidt SA, Chandel NS, Hynes KL, Schumacker PT, Gewertz BL: Endothelial permeability and IL-6 production during hypoxia: role of ROS in signal transduction. Am J Physiol 1999, 277:L1057–L1065
38. Pang C, Gao Z, Yin J, Zhang J, Jia W, Ye J: Macrophage infiltration into adipose tissue may promote angiogenesis for adipose tissue remodeling in obesity. Am J Physiol Endocrinol Metab 2008, 295:E313–E322
39. Siebert M, Krieg P, Lehmann WD, Marks F, Fürstenberger G: Enzymic characterization of epidermis-derived 12-lipoxygenase isoenzymes. Biochem J 2001, 355:97–104
40. Stout RD, Suttles J: Functional plasticity of macrophages: reversible adaptation to changing microenvironments. J Leukoc Biol 2004, 76:509–513

41. VanRollins M, Baker RC, Sprecher HW, Murphy RC: Oxidation of docosahexaenoic acid by rat liver microsomes. J Biol Chem 1984, 259:5776–5783
42. Christmas P, Tolentino K, Primo V, Berry KZ, Murphy RC, Chen M, Lee DM, Soberman RJ: Cytochrome P-450 4F18 is the leukotriene B4 omega-1/omega-2 hydroxylase in mouse polymorphonuclear leukocytes: identification as the functional orthologue of human polymorphonuclear leukocyte CYP4F3A in the down-regulation of responses to LTB4. J Biol Chem 2006, 281:7189–7196
43. Serhan CN, Chiang N, Van Dyke TE: Resolving inflammation: dual anti-inflammatory and pro-resolution lipid mediators. Nat Rev Immunol 2008, 8:349–361
44. Farias SE, Zarini S, Precht T, Murphy RC, Heidenreich KA: Transcellular biosynthesis of cysteinyl leukotrienes in rat neuronal and glial cells. J Neurochem 2007, 103:1310–1318
45. Kapoor M, Kojima F, Appleton I, Kawai S, Crofford LJ: Major enzymatic pathways in dermal wound healing: current understand-ing and future therapeutic targets. Curr Opin Investig Drugs 2006, 7:418–422
46. Kämpfer H, Schmidt R, Geisslinger G, Pfeilschifter J, Frank S: Wound inflammation in diabetic ob/ob mice: functional coupling of prostaglandin biosynthesis to cyclooxygenase-1 activity in diabetes-impaired wound healing. Diabetes 2005, 54:1543–1551
47. Wright E Jr, Scism-Bacon JL, Glass LC: Oxidative stress in type 2 diabetes: the role of fasting and postprandial glycaemia. Int J Clin Pract 2006, 60:308–314
48. Cederbaum SD, Yu H, Grody WW, Kern RM, Yoo P, Iyer RK: Arginases I and II: do their functions overlap? Mol Genet Metab 2004, 81 Suppl 1:S38–S44
49. Li SL, Reddy MA, Cai Q, Meng L, Yuan H, Lanting L, Natarajan R: Enhanced proatherogenic responses in macrophages and vascular smooth muscle cells derived from diabetic db/db mice. Diabetes 2006, 55:2611–2619